NASA Technical Memorandum 106513
ICOMP–94–3; CMOTT–94–1

Modeling of Wall-Bounded Complex Flows and Free Shear Flows

Tsan-Hsing Shih and Jiang Zhu
Institute for Computational Mechanics in Propulsion
and Center for Modeling of Turbulence and Transition
Lewis Research Center
Cleveland, Ohio

and

John L. Lumley
Cornell University
Ithaca, New York

Prepared for the
ASME Fluids Engineering Conference, Symposium on Boundary Layer and Free Shear Flows
sponsored by the American Society of Mechanical Engineers
Lake Tahoe, Nevada, June 19–23, 1994

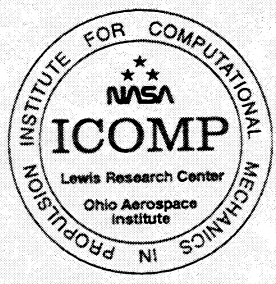

MODELING OF WALL-BOUNDED COMPLEX FLOWS AND FREE SHEAR FLOWS

Tsan-Hsing Shih and Jiang Zhu
Institute for Computational Mechanics in Propulsion
and Center for Modeling of Turbulence and Transition
Lewis Research Center
Cleveland, Ohio 44135

John L. Lumley
Cornell University
Ithaca, New York 14853

ABSTRACT

Various wall-bounded flows with complex geometries and free shear flows have been studied with a newly developed realizable Reynolds stress algebraic equation model. The model development is based on the invariant theory in continuum mechanics. This theory enables us to formulate a general constitutive relation for the Reynolds stresses. Pope (1975) was the first to introduce this kind of constitutive relation to turbulence modeling. In our study, realizability is imposed on the truncated constitutive relation to determine the coefficients so that, unlike the standard k-ε eddy viscosity model, the present model will not produce negative normal stresses in any situations of rapid distortion. The calculations based on the present model have shown encouraging success in modeling complex turbulent flows.

1. INTRODUCTION

The present study concentrates on complex turbulent shear flows which are of great interest in propulsion systems. These flows are backward-facing step flows, confined coflowing jets, confined swirling coaxial jets, U-duct flows and diffuser flows. Most of these flows have complex structures. For example, the confined coflowing jet combines several types of flow structures, such as the shear layer, jet, recirculation, separation and reattachment. Accurate prediction of these flows is of great importance for engine design in all its key elements. Turbulent free shear flows (such as mixing layers, planar and round jets) have been also studied for the purpose of examining the performance of turbulence models in different benchmark flows.

The turbulence model used in this study is a newly developed realizable Reynolds stress algebraic equation model which is fundamentally different from the traditional algebraic Reynolds stress models. The present model is developed using the invariance theory in continuum mechanics. This theory leads to a general constitutive relation for the Reynolds stress tensor $\overline{u_i u_j}$ in terms of the mean deformation rate tensor $U_{i,j}$ and the turbulent velocity and length scales characterized by the turbulent kinetic energy k and its dissipation rate ε. Pope (1975) applied this kind of constitutive relation to Rodi's algebraic Reynolds stress formulation in conjunction with the LRR second order closure model (Launder et al., 1975) and obtained an explicit algebraic expression for the Reynolds stresses for a two-dimensional mean flow field. Taulbee (1992) was able to extend this method to a general three-dimensional flow. We notice that in Rodi's algebraic Reynolds stress formulation, some assumed concepts are in general not valid for most turbulent shear flows, for example, the assumption of constant anisotropy of the Reynolds stresses and neglect of turbulent transport of second moments. These assumptions may bring large errors to turbulence modeling. In addition, an inappropriate second order closure model would also add errors to this type of model. In this study, Rodi's formulation was not used. We directly impose realizability on the constitutive relation for the Reynolds stresses to determine the coefficients in the relation. As a result, a realizable explicit expression for the Reynolds stresses is obtained for general three-dimensional turbulent flows. Some model constants are fine-tuned against a backward-facing step flow and then tested in other flows.

The calculations are performed with a conservative finite volume method (Zhu, 1991). Grid independent and low numerical diffusion solutions are obtained by using differencing schemes of second-order accuracy on sufficiently fine grids. For wall-bounded flows, the standard wall function approach (Launder and Spalding, 1974) is used for wall boundary conditions. The results are compared in detail with experimental data for both mean and turbulent quantities. Calculations using the standard k-ε eddy viscosity model are also carried out for the purpose of comparison. The comparison shows that

the present realizable Reynolds stress algebraic equation model significantly improves the predictive capability of k-ε equation based models, expecially for flows involving massive separations or strong shear layers. In these situations, the standard eddy viscosity model overpredicts the eddy viscosity and, hence, fails to accurately predict wall shear stress, separation, recirculation, etc. We find that the success of the present model in modeling the above mentioned complex flows is largely due to its effective eddy viscosity formulation which accounts for the effect of mean shear rates. According to the present model, the effective eddy viscosity will be significantly reduced by the mean strain rate and maintained at a correct level to mimic the complex flow structures.

2. TURBULENCE MODEL

2.1 Constitutive Relation. Constitutive relations for the Reynolds stresses were derived by several researchers (Pope, 1975, Yoshizawa, 1984 and Rubinstein and Barton, 1990). Shih and Lumley (1993) used the invariant theory in continuum mechanics and the generalized Cayley-Hamilton formulations (Rivlin, 1955) to derive a more (perhaps the most) general constitutive relation for the Reynolds stresses under the assumption that the Reynolds stresses are dependent only on the mean velocity gradients and the characteristic scales of turbulence characterized by the turbulent kinetic energy k and its dissipation rate ε. This relation is

$$\begin{aligned}
\overline{u_i u_j} &= \frac{2}{3}k\delta_{ij} + 2a_2\frac{K^2}{\varepsilon}(U_{i,j}+U_{j,i}-\frac{2}{3}U_{i,i}\delta_{ij}) \\
&+ 2a_4\frac{K^3}{\varepsilon^2}(U_{i,j}^2+U_{j,i}^2-\frac{2}{3}\Pi_1\delta_{ij}) \\
&+ 2a_6\frac{K^3}{\varepsilon^2}(U_{i,k}U_{j,k}-\frac{1}{3}\Pi_2\delta_{ij}) \\
&+ 2a_7\frac{K^3}{\varepsilon^2}(U_{k,i}U_{k,j}-\frac{1}{3}\Pi_2\delta_{ij}) \\
&+ 2a_8\frac{K^4}{\varepsilon^3}(U_{i,k}U_{j,k}^2+U_{i,k}^2U_{j,k}-\frac{2}{3}\Pi_3\delta_{ij}) \\
&+ 2a_{10}\frac{K^4}{\varepsilon^3}(U_{k,i}U_{k,j}^2+U_{k,j}U_{k,i}^2-\frac{2}{3}\Pi_3\delta_{ij}) \\
&+ 2a_{12}\frac{K^5}{\varepsilon^4}(U_{i,k}^2U_{j,k}^2-\frac{1}{3}\Pi_4\delta_{ij}) \\
&+ 2a_{13}\frac{K^5}{\varepsilon^4}(U_{k,i}^2U_{k,j}^2-\frac{1}{3}\Pi_4\delta_{ij}) \\
&+ 2a_{14}\frac{K^5}{\varepsilon^4}(U_{i,k}U_{l,k}U_{l,j}^2+U_{j,k}U_{l,k}U_{l,i}^2-\frac{2}{3}\Pi_5\delta_{ij}) \\
&+ 2a_{16}\frac{K^6}{\varepsilon^5}(U_{i,k}U_{l,k}^2U_{l,j}^2+U_{j,k}U_{l,k}^2U_{l,i}^2-\frac{2}{3}\Pi_6\delta_{ij}) \\
&+ 2a_{18}\frac{K^7}{\varepsilon^6}(U_{i,k}U_{l,k}U_{l,m}^2U_{j,m}^2+U_{j,k}U_{l,k}U_{l,m}^2U_{i,m}^2 \\
&- \frac{2}{3}\Pi_7\delta_{ij}) \qquad (1)
\end{aligned}$$

where

$$\begin{aligned}
&\Pi_1 = U_{i,k}U_{k,i},\ \Pi_2 = U_{i,k}U_{i,k},\ \Pi_3 = U_{i,k}U_{i,k}^2, \\
&\Pi_4 = U_{i,k}^2U_{i,k}^2,\ \Pi_5 = U_{i,k}U_{l,k}U_{l,i}^2,\ \Pi_6 = U_{i,k}U_{l,k}^2U_{l,i}^2, \\
&\Pi_7 = U_{i,k}U_{l,k}U_{l,m}^2U_{i,m}^2 \qquad (2)
\end{aligned}$$

Eq.(1) contains 11 undetermined coefficients which are, in general, scalar functions of various invariants of the tensors in question, for example, $S_{ij}S_{ij}$ (strain rate) and $\Omega_{ij}\Omega_{ij}$ (rotation rate) which are $(\Pi_2+\Pi_1)/2$ and $(\Pi_2-\Pi_1)/2$ respectively. The detailed forms of these scalar functions must be determined by other model constraints such as realizability, and by experimental data.

It is noticed that the standard k-ε eddy viscosity model corresponds to the first two terms on the right hand side of Eq.(1). Both the two-scale direct interaction approximation approach (Yoshizawa, 1984) and the RNG method (Rubinstein and Barton, 1990) also provided a relation which is the first five terms on the right hand side of Eq.(1).

In this study, for simplicity we truncate Eq.(1) to its quadratic tensorial form which is of the same form as those developed by Yoshizawa (1984) and Rubinstein and Barton (1990).

2.2 Realizability. Realizability (Schumann,1977, Lumley,1978), defined as the requirement of the nonnegativity of turbulent normal stresses and Schwarz' inequality between any fluctuating quantities, is a basic physical and mathematical principle that the solution of any turbulence model equation should obey. It also represents a minimal requirement to prevent a turbulence model from producing unphysical results. In the following, this principle will be applied to the truncated constitutive relation Eq.(1) to derive constraints on its coefficients.

Let us first consider a two-dimensional pure mean deformation in which the deformation rate tensor contains only non-zero diagonal components, i.e.,

$$U_{i,j} = 0, \quad \text{if} \quad i \neq j$$

In this case, the normal stress $\overline{u_1u_1}$ can be written as

$$\frac{\overline{u_1u_1}}{2k} = \frac{1}{3} + 2a_2\frac{k}{\varepsilon}U_{1,1} + \frac{1}{3}(2a_4+a_6+a_7)\frac{k^2}{\varepsilon^2}(U_{1,1})^2$$

If we define a time scale ratio of the turbulent to the mean strain rate as $\eta = S\ k/\varepsilon$, where $S = \sqrt{2S_{ij}S_{ij}}$, the above equation can be written as

$$\frac{\overline{u_1u_1}}{2k} = \frac{1}{3} + a_2\eta + \frac{1}{12}(2a_4 + a_6 + a_7)\eta^2$$

Physically, we know that $\overline{u_1u_1}$ will decrease due to the stretching by $U_{1,1}$. However, by realizability $\overline{u_1u_1}$ should not be driven to negative values. Therefore, we require that

$$\frac{\overline{u_1u_1}}{2k} \to 0, \qquad \text{if } \eta \to \infty$$
$$(\frac{\overline{u_1u_1}}{2k})_{,\eta} \to 0, \qquad \text{if } \eta \to \infty$$

These physically necessary conditions are called the realizability conditions. Similar analysis of $\overline{u_2u_2}$ and $\overline{u_3u_3}$ also leads to the above conditions. In addition, it should be mentioned that the above analysis also holds for the situation of a three-dimensional pure strain rate. These conditions can be satisfied in several ways. Among them the simplest way is perhaps the following:

$$2a_2 = -\frac{2/3}{A_1 + \eta}$$
$$2a_4 = \frac{C_{\tau 1}}{A_2 + \eta^3 + \xi^3}$$
$$2a_6 = \frac{C_{\tau 2}}{A_2 + \eta^3 + \xi^3}$$
$$2a_7 = \frac{C_{\tau 3}}{A_2 + \eta^3 + \xi^3}$$

where $\xi = \Omega k/\varepsilon$, $\Omega = (2\Omega^*_{ij}\Omega^*_{ij})^{1/2}$, $\Omega^*_{ij} = (U_{i,j} - U_{j,i})/2 + 4\varepsilon_{mji}\omega_m$ and ω_m represents the rotation of the coordinate frame. $A_1, A_2, C_{\tau 1}, C_{\tau 2}$ and $C_{\tau 3}$ will be taken as constants and determined by comparing calculations with experiments.

It can be seen from the above analysis that realizability cannot be fully satisfied if the model coefficients (a_2-a_7) are taken as constant, such as those in the standard k-ε model and some anisotropic models, such as the model of Speziale (1987). In fact, these models satisfy realizability only in the weak sense, i.e., they only ensure the positivity of the sum of the normal Reynolds stresses. For more detailed discussion about model coefficients see Shih *et al.*(1993).

2.3 Model Equations. The realizable Reynolds stress algebraic equation model can be written as

$$\overline{u_iu_j} = \frac{2}{3}k\delta_{ij} - \nu_t(U_{i,j} + U_{j,i})$$
$$+ \frac{C_{\tau 1}}{A_2 + \eta^3 + \xi^3}\frac{k^3}{\varepsilon^2}(U_{i,k}U_{k,j} + U_{j,k}U_{k,i} - \frac{2}{3}\Pi_1\delta_{ij})$$
$$+ \frac{C_{\tau 2}}{A_2 + \eta^3 + \xi^3}\frac{k^3}{\varepsilon^2}(U_{i,k}U_{j,k} - \frac{1}{3}\Pi_2\delta_{ij})$$
$$+ \frac{C_{\tau 3}}{A_2 + \eta^3 + \xi^3}\frac{k^3}{\varepsilon^2}(U_{k,i}U_{k,j} - \frac{1}{3}\Pi_2\delta_{ij}) \qquad (3)$$

Two quantities, the turbulent kinetic energy k and its dissipation rate ε, remain to be determined in Eq.(3). To this end, we use the standard k-ε model equations which are

$$k_{,t} + U_jk_{,j} = [(\nu + \frac{\nu_t}{\sigma_K})k_{,j}]_{,j} - \overline{u_iu_j}U_{i,j} - \varepsilon$$
$$\varepsilon_{,t} + U_j\varepsilon_{,j} = [(\nu + \frac{\nu_t}{\sigma_\varepsilon})\varepsilon_{,j}]_{,j} - C_{\varepsilon 1}\frac{\varepsilon}{k}\overline{u_iu_j}U_{i,j} - C_{\varepsilon 2}\frac{\varepsilon^2}{k}$$

where

$$\nu_t = C_\mu\frac{k^2}{\varepsilon}, \qquad C_\mu = \frac{2/3}{A_1 + \eta}$$

The coefficients $C_{\varepsilon 1}, C_{\varepsilon 2}, \sigma_K$ and σ_ε assume their standard values:

$$C_{\varepsilon 1} = 1.44, \quad C_{\varepsilon 2} = 1.92, \quad \sigma_K = 1, \quad \sigma_\varepsilon = 1.3$$

and the other coefficients are taken as

$$C_{\tau 1} = -4,\ C_{\tau 2} = 13,\ C_{\tau 3} = -2,\ A_1 = 5.5,\ A_2 = 1000.$$

These values are calibrated against the backward-facing step flow of Driver and Seegmiller (1985) for which a complete set of experimental data is available for both mean and turbulent quantities and they are also found to be appropriate for other complex flows studied in this work.

3. APPLICATIONS

3.1 Diffuser Flows. Two conical diffuser flows were calculated, one with a 8° total angle (Trupp et al., 1986) and the other 10° (Fraser, 1958). In both cases, the flows undergo strong adverse pressure gradients but remain attached. Although the flow configuration looks simple, it is not easy to calculate this type of flow accurately, especially for the boundary layer quantities. Fig.1 shows the variation of calculated and measured wall friction coefficient C_f with the axial distance x/R_o (R_o is the inlet duct radius). It is seen that the result of the present model is in good agreement with the experimental data, while the standard k-ε (SKE) model overpredicts C_f along almost the entire length of the diffuser. The calculated and measured displacement

thickness δ^* are compared in Fig.2. The comparison shows that the SKE model gives a good prediction in the upstream region, but deviates significantly from the experiment downstream; the present model prediction is good in the whole region. Fig.3 shows the comparison of calculated and measured shape factor H. This is the case in which the worst agreement with the measurement has been found for both models. Nevertheless, the present model still performs considerably better than does the SKE model.

3.2 U-Duct Flow. This case is the experiment of Monson et al. (1990) conducted in a 180° planar turnaround duct. It features flow with large streamline curvature. Calculations are compared to the experiment taken at a flow Reynolds number of 10^6. Fig.4 shows the streamlines computed with the present model. A small separation region is found at the bend exit. However, the SKE model does not predict the flow separation. Fig.5 shows the comparison of calculated and measured C_f along the inner wall. The bend is located between $21.7 \leq s/H \leq 24.8$. Both models are seen to behave in the same manner and produce large discrepancies in the bend region. The reason for this may partially due to the use of the wall function which does not respond to the severe pressure gradient.

3.3 Backward-Facing Step Flows. Two backward facing step flows, measured by Driver and Seegmiller (1985) and Kim et al. (1978), were calculated. The former (DS case) has a smaller and the latter (KKJ case) a larger step expansion. The computed and measured reattachment points are compared in Table 1. The calculated reattachment point from the present model agrees well with the experiments. Fig.6 shows the comparison of the computed and the measured static pressure coefficient C_p along the bottom wall. The SKE model is seen to predict a premature pressure rise, which is consistent with its underprediction of the reattachment length, while the present model captures the pressure rise quite well. Fig.7 shows the comparisons of predicted and measured turbulent stresses $\overline{uu}$, $\overline{vv}$ and $\overline{uv}$ at the location x=2 which is in the recirculation region. In the KKJ-case, no reliable experimental data exist for the turbulent stresses due to the unsteadiness of the flow. However, the experimental data of the DS-case is considered more reliable because of the smaller unsteadiness of the flow. As compared with the results of the SKE model in Fig.7, it is seen that the anisotropic terms in the present model increase $\overline{uu}$ and decrease $\overline{vv}$, leading to significant improvements in both $\overline{uu}$ and $\overline{vv}$ except in the near-wall region. On the other hand, the anisotropic terms have little impact on $\overline{uv}$. The improvement obtained by the present model for $\overline{uv}$ is mainly due to the reduction in C_μ by strain rate.

Table 1. Comparison of the reattachment points

Case	measurement	SKE	PRESENT
DS	6.1	4.99	5.82
KKJ	7± 0.5	6.35	7.35

3.4 Confined Jets. The general features of confined jets, the experiments of Barchilon and Curtet (1964), are sketched in Fig.8. At the entrance, two uniform flows, a jet of larger velocity and an ambient stream of smaller velocity, are discharged into a cylindrical duct of diameter D_o. The inlet flow conditions can be characterized by the Craya-Curtet number C_t. The experiment shows that recirculation occurs when $C_t < 0.96$. For a given geometry, recirculation as well as adverse pressure gradients can be intensified by reducing the value of C_t at the entrance. The separation and reattachment points of the predicted recirculation bubbles are compared with the experimental data in Fig.9. The experiment indicated that as C_t decreases, the separation point moves upstream while the reattachment point remains practically unchanged. The present model captures this feature well and predicts both the separation and reattachment points much better than does the SKE model. The variation of the pressure coefficient C_p along the duct wall is shown in Fig.10. The pressure distribution is governed by the jet entrainment as well as the contraction and expansion of the flow caused by the recirculation bubble. The decrease in the ambient velocity induced by the entrainment gives rise to an adverse pressure gradient, while the contraction of streamlines produces the opposite effect. These two mechanisms interact more intensely with each other as C_t decreases and cause the pressure to vary little in the region upstream of the center of the recirculation bubble. However, in the downstream part of the recirculation bubble, the deceleration of the flow sets up an adverse pressure gradient, the slope of which becomes steeper as C_t decreases. Therefore, the ability to capture the location of the recirculation center will have a direct impact on the prediction of the pressure. Regarding the comparison between predictions and experiments, it is seen that

although both models predict practically the same total pressure rises which are in excellent agreement with the measurements, the present model captures the steep pressure gradients better than does the SKE model for all of the C_t values.

3.5 Confined Swirling Coaxial Jets. This is the case experimentally studied by Roback and Johnson (1983). Fig.11 shows the general features of the flow. At the inlet, an inner jet and an annular jet are ejected into an enlarged duct. Besides an annular recirculation bubble due to sudden expansion of the duct, a centerline recirculation bubble is created by flow swirling. Fig.12 compares the calculation of the centerline velocity with the experiment. The negative velocity indicates the central recirculation. It is seen that both models predict the strength of central recirculation and the front stagnation point quite well, but the present model predicts the rear stagnation point much better than does the SKE model. Fig.13 shows the comparison of calculated and measured mean velocity profiles at x=5.1cm. Both models give reasonably good profiles which are within experimental scatter, except for the peak values of the axial and radial velocities. Both models have been found to give nearly the same results in the downstream region, which can also be seen from Fig.12.

3.6 Turbulent Free Shear Flows. Calculations were also performed for a mixing layer, a plane and a round jet. The results shown here are only for the jets due to the space limitation. Figs.14 and 15 show the comparisons of the self-similar mean velocity profiles from the model predictions and the various measurements for the plane and round jets, respectively. In Fig.14, the model predictions are compared with the measurement of Gutmark and Wygnanski (1976) for the plane jet. The predictions given by both the present model and the SKE model agree well with the experimental data. For the round jet, the comparisons are made between the model predictions and the measurements of Rodi (1975) and are shown in Fig.15. The profile distribution of the mean velocity predicted by the present model agrees well with Rodi's data, while the SKE model predicts a faster spreading of the round jet into the surroundings and a wider distribution.

4. CONCLUSION

A realizable Reynolds stress equation model has been applied to calculate both complex wall bounded flows and free shear flows. The calculations have been compared with available experimental data. The comparisons show that the present model provides significant improvement over the standard k-ε eddy viscosity model and that the present model is robust and economical as well. This indicates that the present model has good potential to be a practical tool in engineering applications.

ACKNOWLEDGEMENTS

The authors are grateful to Drs. Z. Yang and W.W. Liou for their calculations of free shear flows and fruitful discussions. The work of J.L. Lumley was supported in part by Contract No. AFOSR 89-0226, jointly funded by the U.S. Air Force Office of Scientific Research (Control and Aerospace Programs), and the U.S. Office of Naval Research, and in part by Grant No. F49620-92-J-0038, funded by the U.S. Air Force Office of Scientific Research.

REFERENCES

Barchilon, M., and Curtet, R., 1964, "Some details of the structure of an axisymmetric confined jet with backflow," *J. Basic Eng.*, Vol.86, pp.777-787.

Driver, D.M. and Seegmiller, H.L., 1985, "Features of a reattaching turbulent shear layer in divergent channel flow," *AIAA J.*, Vol.23, pp.163-171.

Fraser, H.R., 1958, "The turbulent boundary layer in a conical diffuser," *J. Hydraulics Division*, pp.1684.1-1684.17.

Gutmark, E. and Wygnanski, I., 1976, "The planar turbulent jet," *J. Fluid Mech.*, Vol.73, pp.465-495.

Kim, J., Kline, S.J. and Johnston, J.P., 1978, "Investigation of separation and reattachment of a turbulent shear layer: Flow over a backward-facing step," Rept. MD-37, Thermosciences Div., Dept. of Mech. Eng., Stanford University.

Launder, B.E., Reece, G.J. and Rodi, W., 1975, "Progress in the development of a Reynolds-stress turbulence closure," *J. Fluid Mech.*, Vol.68, pp.537-566.

Launder,B.E. and Spalding,D.B., 1974, "The numerical computation of turbulent flows," *Comput. Methods Appl. Mech. Eng.*, Vol.3, pp.269-289.

Lumley, J.L., 1978, "Computational modeling of turbulent flows," *Adv. Appl. Mech.*, Vol.18, pp.124-176.

Monson, D.J., Seegmiller, H.L., McConnaughey, P.K. and Chen, Y.S., 1990, "Comparison of experiment with calculations using curvature-corrected zero and two

equation turbulence models for a two-dimensional U-duct," AIAA Paper 90-1484.

Pope, S.B., 1975, "A more general effective-viscosity hypothesis," *J. Fluid Mech.*, Vol.72, pp.331-340.

Rivlin, R.S., 1955, "Further remarks on the stress deformation relations for isotropic materials", *J. Arch. Ratl. Mech. Anal.*, Vol.4, pp.681-702.

Roback, R. and Johnson, B.V., 1983, "Mass and momentum turbulent transport experiments with confined swirling coaxial jets," NASA CR 168252.

Rodi, W., 1975, "A new method of analyzing hot-wire signals in highly turbulent flow and its evaluation in round jets," Disa Information, No.17.

Rubinstein, R. and Barton, J.M., 1990, "Nonlinear Reynolds stress models and the renormalization group," *Phys. Fluids A*, Vol.2, pp.1472-1476.

Schumann, U., 1977, "Realizability of Reynolds stress turbulence models," *Phys. Fluids*, Vol.20, pp.721-725.

Shih, T.-H. and Lumley, J.L., 1993, "Remarks on turbulent constitutive relations," *Math. Comput. Modelling*, Vol.18, pp.9-16.

Shih, T.-H., Zhu, J., and Lumley, J.L., 1993, "A realizable Reynolds stress algebraic equation model," NASA TM 105993.

Speziale, C.G., 1987, "On nonlinear K-l and K-ϵ models of turbulence," *J. Fluid Mech.*, Vol.178, pp.459-475.

Taulbee,D.B., 1992,"An improved algebraic Reynolds stress model and corresponding nonlinear stress model," *Phys. Fluids A*, Vol.4, pp.2555-2561.

Trupp, A.C., Azad, R.S. and Kassab, S.Z., 1986, "Near-wall velocity distributions within a straight conical diffuser," *Exps. Fluids*, Vol.4, pp.319-331.

Yoshizawa,A., 1984,"Statistical analysis of the derivation of the Reynolds stress from its eddy-viscosity representation," *Phys. Fluids*, Vol.27, pp.1377-1387.

Zhu, J., 1991, "FAST-2D: A computer program for numerical simulation of two-dimensional incompressible flows with complex boundaries," Rept. No.690, Institute for Hydromechanics, University of Karlsruhe.

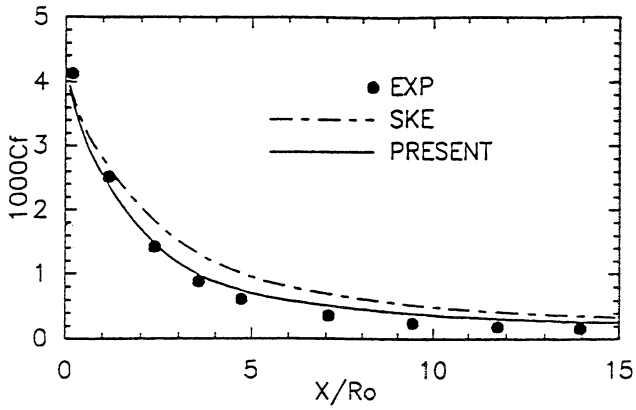

Fig.1 Wall friction coefficient (Case of Trupp et al.)

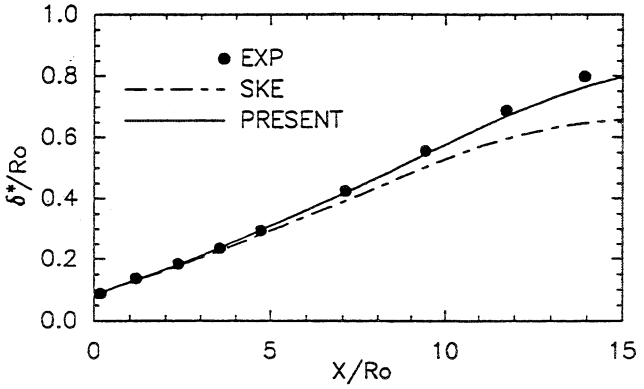

Fig.2 Displacement thickness (Case of Trupp et al.)

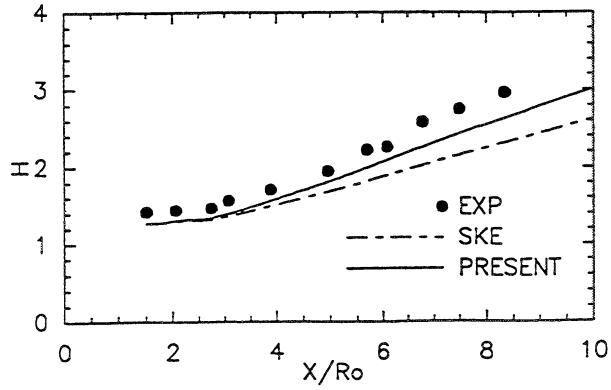

Fig.3 Shape factor (Case of Fraser)

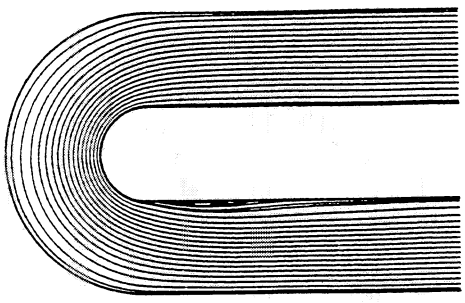

Fig.4 Streamlines

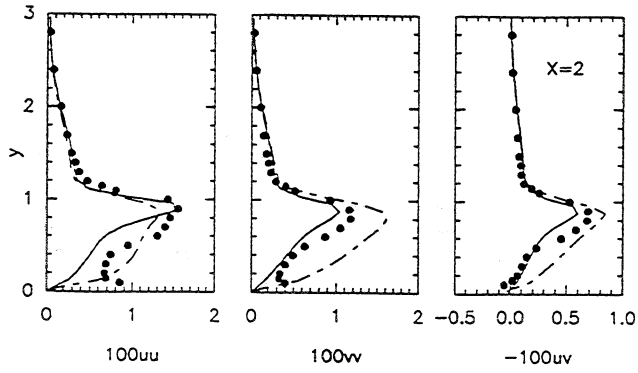

Fig.7 Turbulent stress profiles
(legend as in Fig.5)

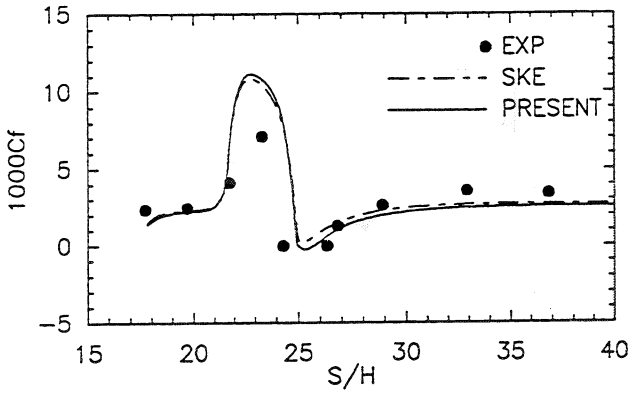

Fig.5 Friction coefficient along the inner wall

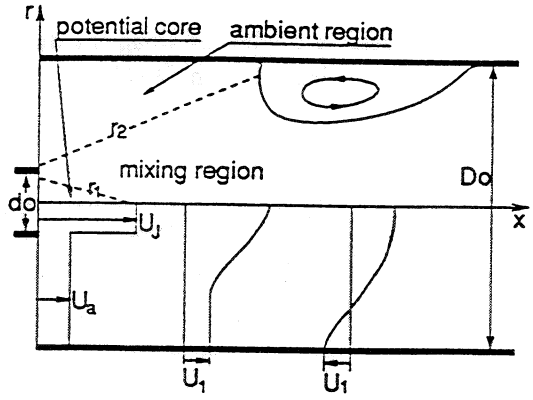

Fig.8 Flow configuration and notations

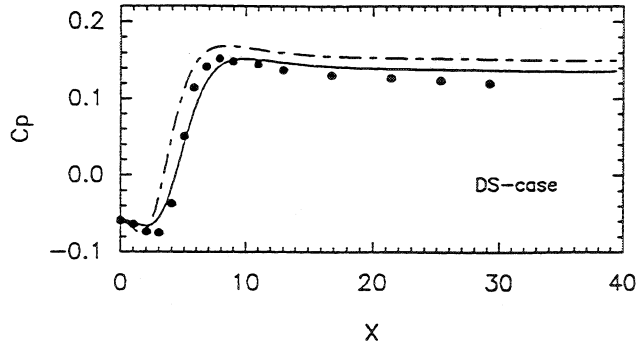

Fig.6 Pressure coefficient along the bottom wall
(legend as in Fig.5)

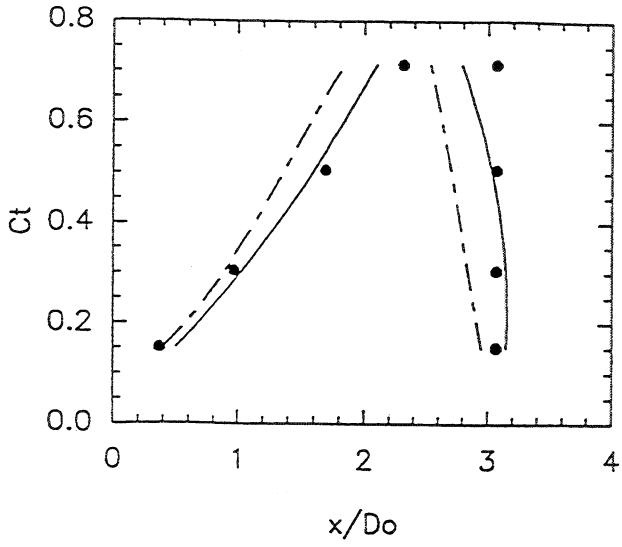

Fig.9 Separation and reattachment points
(legend as in Fig.5)

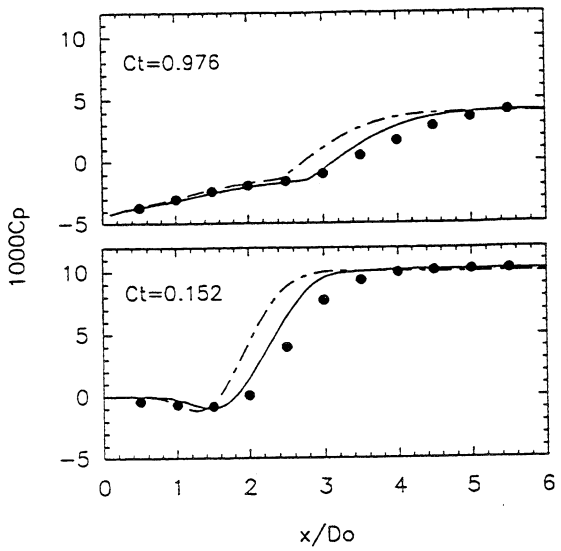

Fig.10 Pressure coefficient along the duct wall (legend as in Fig.5)

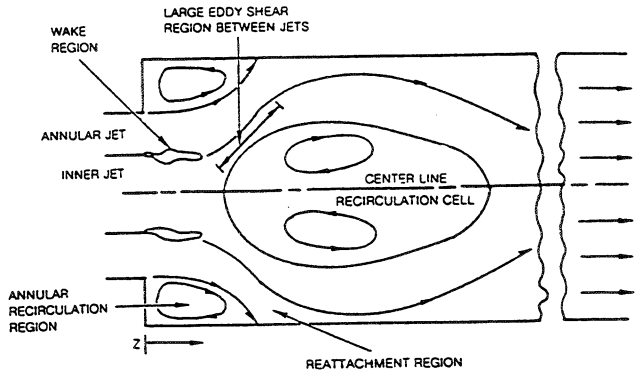

Fig.11 Flow configuration

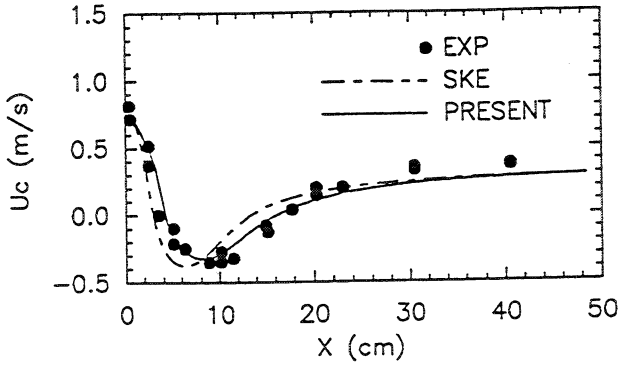

Fig.12 Centerline velocity

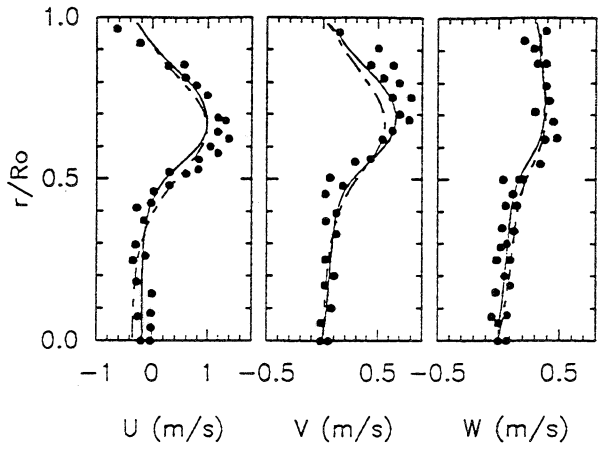

Fig.13 Mean velocity profiles at x=5.1cm (legend as in Fig.12)

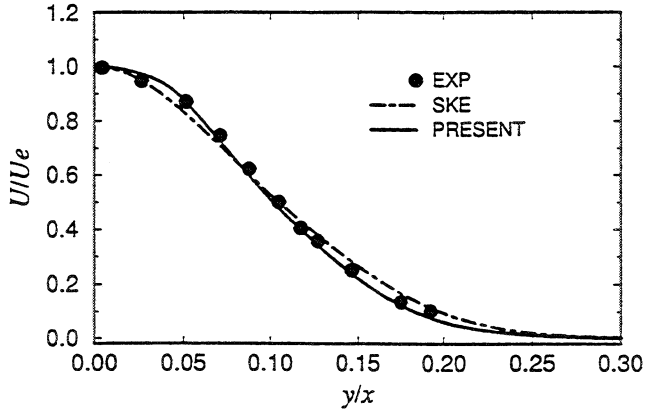

Fig.14 Self-similar mean velocity profiles for plane jet

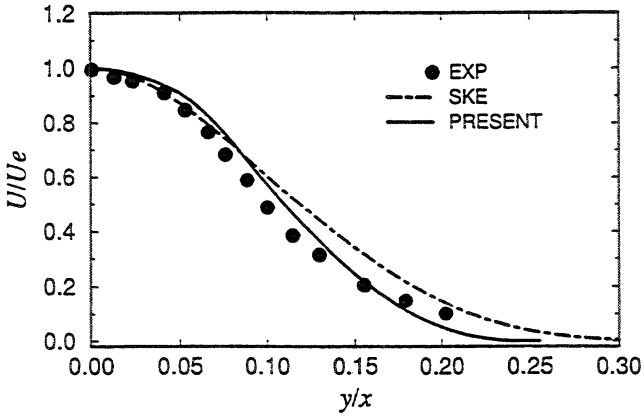

Fig.15 Self-similar mean velocity profiles for round jet

REPORT DOCUMENTATION PAGE

Form Approved
OMB No. 0704-0188

1. AGENCY USE ONLY (*Leave blank*)	2. REPORT DATE	3. REPORT TYPE AND DATES COVERED
	February 1994	Technical Memorandum

4. TITLE AND SUBTITLE

Modeling of Wall-Bounded Complex Flows and Free Shear Flows

5. FUNDING NUMBERS

WU-505-90-5K

6. AUTHOR(S)

Tsan-Hsing Shih, Jiang Zhu, and John L. Lumley

7. PERFORMING ORGANIZATION NAME(S) AND ADDRESS(ES)

National Aeronautics and Space Administration
Lewis Research Center
Cleveland, Ohio 44135-3191

8. PERFORMING ORGANIZATION REPORT NUMBER

E-8624

9. SPONSORING/MONITORING AGENCY NAME(S) AND ADDRESS(ES)

National Aeronautics and Space Administration
Washington, D.C. 20546-0001

10. SPONSORING/MONITORING AGENCY REPORT NUMBER

NASA TM-106513
ICOMP-94-3; CMOTT-94-1

11. SUPPLEMENTARY NOTES

Prepared for the ASME Fluids Engineering Conference, Symposium on Boundary Layer and Free Shear Flows sponsored by the American Society of Mechanical Engineers, Lake Tahoe, Nevada, June 19–23, 1994. Tsan-Hsing Shih and Jiang Zhu, Institute for Computational Mechanics in Propulsion and Center for Modeling of Turbulence and Transition, NASA Lewis Research Center, (work funded under NASA Cooperative Agreement NCC3-233), and John L. Lumley, Cornell University, Ithaca, New York 14853. ICOMP Program Director, Louis A. Povinelli, organization code 2600, (216) 433-5818.

12a. DISTRIBUTION/AVAILABILITY STATEMENT

Unclassified - Unlimited
Subject Category 34

12b. DISTRIBUTION CODE

13. ABSTRACT ***(Maximum 200 words)***

Various wall-bounded flows with complex geometries and free shear flows have been studied with a newly developed realizable Reynolds stress algebraic equation model. The model development is based on the invariant theory in continuum mechanics. This theory enables us to formulate a general constitutive relation for the Reynolds stresses. Pope (1975) was the first to introduce this kind of constitutive relation to turbulence modeling. In our study, realizability is imposed on the truncated constitutive relation to determine the coefficients so that, unlike the standard k-ε eddy viscosity model, the present model will not produce negative normal stresses in any situations of rapid distortion. The calculations based on the present model have shown an encouraging success in modeling complex turbulent flows.

14. SUBJECT TERMS

Turbulence modeling; Separation; Adverse pressure gradient

15. NUMBER OF PAGES

10

16. PRICE CODE

A02

17. SECURITY CLASSIFICATION OF REPORT	18. SECURITY CLASSIFICATION OF THIS PAGE	19. SECURITY CLASSIFICATION OF ABSTRACT	20. LIMITATION OF ABSTRACT
Unclassified	Unclassified	Unclassified	